A modelling approach to the dynamics of gait initiation

Manish Anand
School of Mechanical Engineering
585 Purdue Mall
Purdue University
West Lafayette, IN, USA
Email: manand@purdue.edu

Justin Seipel
School of Mechanical Engineering
585 Purdue Mall
Purdue University
West Lafayette, IN, USA

Shirley Rietdyk
Department of Health and Kinesiology
800 West Stadium Avenue
Purdue University
West Lafayette, IN, USA

ABSTRACT

Gait initiation is an integral and complex part of human locomotion. In this paper, we present a novel compliant-leg model-based approach to understanding the key phases of initiation, the nature of the effective forces involved in initiation, and the importance of the anticipatory postural adjustments (APAs). The results demonstrate that in the presence of APAs, we observe a change in the characteristic of forcing required for initiation, and the energetic cost of gait initiation is also reduced by ~58%. APAs also result in biologically relevant leg landing angles and trajectories of motion. Furthermore, we find that a sublinear functional relationship with the velocity error from steady state predicts the required force, consistent with an open loop control law basis for gait initiation.

Keywords: Gait Initiation. Locomotion, SLIP, open loop

1. INTRODUCTION

Humans regularly perform unsteady dynamic motions. One of the most commonly performed transient motions is gait initiation. Currently, empirical descriptions of gait initiation exist which imply that organizing principles may exist to explain gait initiation (e.g. [1,2]), however, a mechanism and theoretical explanation for this behavior is currently lacking.

Mechanistically, a key characteristic observed in the process of moment generation and gait initiation is that before the first step, the center of pressure (CoP) moves from anterior to posterior direction causing the center of mass (CoM) to undergo an assisted fall-like behavior [3–5]. It has also been demonstrated that gait initiation is a function of the biomechanical constants of the person initiating movement [4]. In this study an inverted pendulum was used to explain the observed relationship between invariance of the time of gait initiation under varying target speeds and step lengths. The authors concluded that gait initiation was almost a pulse control

process with an initial fall phase to generate momentum followed by the controlled gait initiation process that is invariant in time and independent of the targeted steady state speed or step length chosen.

Gait initiation is a transient process which is achieved in a principled controlled manner [6]. Some of the previous literature focused on the first two steps and concluded that since the velocity at the end of first step is ~90% of the mean velocity of progression in the second step, gait was initiated within 1 [7] or 2 steps [3]. However, based on [6,8] it can be concluded that steady state gait is achieved over 3 to 5 steps from initiation. In [6] it was demonstrated that the underlying control process among different age groups might be similar based on the effective dynamics of the bodies, represented by the pattern of mean velocity of progression for each step, being relatively similar. This is also in agreement with [5] where it was shown that there is a baseline motor control for gait initiation which undergoes age related changes resulting in changes to the gait initiation characteristics but the fundamental behavior remains the same. In [8], the use of foot orthoses as opposed to barefoot walking caused a difference in the number of steps to achieve steady state. Both these studies [6,8] relied on direct measurement of CoM kinematics for more than two steps and based their results on mean velocities of progression for all steps to establish steady state, providing a more comprehensive view of the kinematics of gait initiation.

The relevance of gait initiation is well recognized. Existing experimental research considers multiple measures to assess the underlying principles of gait initiation (such as relationships between CoM and CoP [3,4], first step variability [9], and momentum generation relationship to CoP and CoM [5]). Additionally, anticipatory postural adjustments (APAs), including activation of the tibialis anterior (TA) and relaxation of soleus [10] have been shown to

be present invariantly across all subjects [3,10,11]. The APAs manifest in the mechanics of the motion as movement of CoP of the stance leg backwards [3,4,12] before the motion starts. As the CoM begins to move forward, the CoP quickly accelerates back to the center of the stance leg. It has been stated that gait initiation cannot take place without an offset between CoM and CoP, which creates an assisting gravitational moment [3].

In this paper, an open loop inverted pendulum basis has been used to explore the process of gait initiation. Our hypothesis is that the kinematics of gait initiation depend strongly on both applied forcing and the leg landing angle. We expect that gait initiation can be achieved by a strategy as simple as constant forcing, but for the kinematics to be biologically representative and to achieve a steady state quickly, the forcing must be set to a different constant for each step. We further expect that effective imbalances induced by anticipatory postural adjustments (APAs) will modify the forcing and speed changes with each step. We expect system energetic cost associated with the initiation process to be lower in the presence of APAs. A further comparison of the forcing characteristics employed in both the absence and presence of APAs will show that such actions are an integral part of the process. Finally, we will demonstrate that an open-loop control basis for the task of gait initiation can be generated which ties in with both the leg properties and the initial APAs allowing a calculation of the per step force progression ahead of the start of motion. If these are proven to be true, then that suggests a compelling case that gait initiation can be controlled by proactive processes.

1. METHODS

The process of gait initiation will be discussed in the scope of transitioning from standing to walking. The characteristics of the human legs during walking and running can be modeled as

effective leg properties [13–15] (Figure 1). The radial component of ground reaction force approximates a spring like function [15] and exhibits common effective leg properties [16]. The rotary component of ground reaction force has been shown to be important for modeling of biological systems as well as a strategy for robotic platforms [16–18], and in both cases provides a propulsive force. Leg touchdown angle has been shown to be another critical component of steady state locomotion [16–19] and simple leg placement control policies can significantly benefit stability of locomotion with respect to perturbations [19]. The step length associated with gait initiation is a function of touchdown angle [6]. The forcing and energy consumption for steady state motion is also a function of landing angles [15,18].

The bipedal Spring-Loaded Inverted Pendulum (SLIP) model has been established based on the spring like properties exhibited during both walking and running [15]. The rotary component of forcing has been added to the SLIP model, often as a hip moment [18], frequently kept constant for simple control of locomotion. This model has demonstrated significantly improved stability and robustness properties [17–20]. The leg is modelled as a viscoelastic element. The bipedal model used in this study is based on proactive feed-forward forcing. Robots have demonstrated that a significant degree of stability can be achieved without active feedback to control effective leg properties [21]. In fact, experimental studies conclude that gait initiation is a “pre-programmed” task consistent with a feed-forward mode of neural control [11,22]. Therefore, current theory and simple physical models of walking and running clearly indicate that there is a baseline level of stability that is possible with “open-loop” or “proactive” approaches [18,23]. In context of the current research, maintaining a constant level of forcing as is, or following a predetermined forcing level, both are considered as proactive forcing.

1.1 An extension of the bipedal SLIP model:

Here we use an actuated bipedal SLIP model, which is itself an extension of the monopedal hip actuated SLIP model for running [18] and draws some inspiration from the simple bipedal compliant leg model [15]. The addition of a second leg allows the system to exhibit walking behavior with double stance (also termed double support phase). The compliant leg represents the virtual leg mapped between the hip joint and the center of pressure of the corresponding foot. The original hip actuated SLIP model has a constant hip torque which translates to a rotary force which changes with leg length. For the analysis in this paper, we used a model with a rotary force $F_{(T)}$ which represents the effective time averaged rotary force acting on the CoM, instead of a constant hip moment. This means that $F_{(T)}$ remains constant throughout each stance phase. The primary motivation behind this is that there are limitations to relating experimental measures and joint moments to single net effective moment models like hip actuated SLIP. With rotary forcing in play, we can directly look at the resultant component of the ground reaction forces (GRF) from experimental data and make comparisons (as presented in Appendix 5.1). Joint moments are still important for analysis and can be calculated further from the total ground reaction force data and the joint kinematics.

1.1.1 Equations of motion

Force on the CoM due to viscoelastic properties of the leg, acting along the leg (refer Figure 2):

$$F_{(L)} = k(l_0 - l) - c[v_y \cos(\Phi) - v_x \sin(\Phi)]$$

Force perpendicular to leg

$$F_{(T)} = K_0 \text{ (const.)} \qquad \text{(Rotary Force Actuated)}$$

$$\ddot{x} = \frac{1}{m}\sum (F_{(T)i}\cos(\Phi_i) + F_{(L)i}\sin(\Phi_i))$$

$$\ddot{y} = \frac{1}{m}(\Sigma(F_{(L)i}\cos(\Phi_i) - F_{(T)i}\sin(\Phi_i)) - g$$

Table 1 lists the respective leg properties with the associated symbols

i	Left, Right	**c**	Linear damping along the leg
m	Mass of body	**k**	Leg stiffness
V	Velocity of CoM in Cartesian coordinates	**Φ**	Stance leg angle with the vertical
l	Instantaneous leg length	$\mathbf{l_0}$	Nominal Leg Length

Table 1. Leg properties and associated symbols

1.2 Non Dimensionalizations

In order to generalize the model results and compare to biological results, the following non dimensionalization were utilized:

Normalized Speed (statures/sec)

$$\tilde{v} = v/(2l_0)$$

Nondimensionalized Force

$$\tilde{F} = F/(mg)$$

Relative Stiffness

$$K_{REL} = kl_0/(mg)$$

Damping Ratio

$$\varsigma = c/(2\sqrt{mk})$$

1.3 Cost of Gait Initiation

In locomotion studies, the cost of transport (COT) at steady state is a measure of efficiency of the motion. For transient motion, we can define a similar cost of transport which measures the energetic cost of motion until steady state is achieved. We have termed this the cost of gait initiation (CGI).

$$CGI = \frac{E_N}{mgd}$$

where E_N is the sum total of initial kinetic energy and energy consumed in N steps, and d is the forward displacement of the body in those N steps. The initial kinetic energy accounts for the energy added due to the APAs and is added until the first lift-off. A horizontal translation of the COM is assumed during this period implying that there is no change in the potential energy. Hence, the total energy exchange during this period is the gain in kinetic energy. This metric will be used to compare multiple strategies of gait initiation.

This manuscript includes three studies in which the model characteristics become progressively more complex. In Study 1, the constant rotary force is the same at each step, and the experimental and modeling kinematics are compared to determine adequacy of this simple control process. In Study 2, the constant rotary force is adjusted such that a different constant force is applied at each successive step. The applied forcing, CoM trajectories, and CGI are examined as a function of leg angle to determine the model leg landing angle that best matches the experimental data. In Study 3, an APA is added to determine how the leg landing angle is affected, and to determine if an APA changes the required forcing pattern and reduces the CGI.

2. RESULTS

2.1 Gait Initiation with Constant Rotary Forcing:

Overall, simulations of the actuated bipedal SLIP model reveal that stable gait initiation from a state of rest can be achieved by applying a constant rotary force, effective leg stiffness, and leg landing angle. We calculated the constant forcing required at steady state to maintain the target velocity, then applied this force as a constant for every step throughout the gait initiation process. The model does transition to a steady state, indicating that the system can stably attract to steady behavior with this very simple "proactive" approach where all system properties are controlled to be constant. The kinematics of the CoM are, however, significantly different from those observed experimentally. The model required 15 or more steps for the CoM to reach steady state, as opposed to three steps observed experimentally ([6];Figure 3)

This implies that there is a higher level of control or planning necessary to achieve steady state as rapidly as observed in human experiments.

2.2 Step Specific Rotary Force Characteristics for Gait Initiation:

In a second study, we allowed the forcing level applied each step to change from step to step. We calculated the rotary force required at each step, in order to produce the same forward velocity profile as found during human experiments (Figure 4a). For a fixed leg stiffness ($k=20000\ Nm^{-1}$, $K_{REL} = 29$) and leg damping ($c=950\ Nsm^{-1}$,$\zeta=0.34$) that are representative of human gait[15,24], as well as a fixed leg landing angle, we computed the rotary force required for each step of the gait initiation. We then re-computed this for multiple leg landing angles (of which, results for 70°, 66°, and 61° are presented in Figure 4 (b), (c) and (d) respectively). The per step rotary forcing sequence is fixed from the beginning of gait initiation.

We find that there exists a stark difference between these solutions (Figure 4 (b), (c) and

(d)). Particularly, a higher average rotary forcing is required throughout gait initiation for smaller landing angles (Figure 4 (d)). Also, as the landing angle is changed, the pattern of forcing levels from step to step changes in a nonlinear manner. For landing angles ~70°, the forcing pattern is oscillatory with large magnitude forces at the initial and every alternate step (>0.2 BW) and smaller values at every even step (~1-35% of the forcing in the initial step) (Figure 4 (b)). As landing angle decreases, the oscillations in forces is reduced and the magnitudes of forces become more consistent (Figure 4 (c)) until we reach a landing angle of 61° at which the forces at each step are comparable throughout all steps (Figure 4 (d)). This solution is of particular interest as it achieves a steady state in the third step itself implying that this is forcing characteristic to be applied to match the experimentally observed gait initiation behavior.

The comparison of these forcing patterns highlights the sensitivity of the solution to landing angle. This also implies that even though the average forward velocity becomes constant after the third step, large changes in actuation are required to maintain a constant forward velocity at steeper landing angles (e.g. 70°). Despite the average forward velocities being the same for all three values of leg landing angles, the CoM kinematics are not similar (Figure 5). The CoM vertical displacement more than doubled (~4 vs 10 cm) as the leg angle changed from 70° to 66°. Further, it is visually apparent the CoM vertical displacement is smoother for 70° than for 66° or 61°.

Steady State Solution: There are multiple strategies or ways to achieve the same pattern of speed progression as found in human experiments. However, these strategies differ widely in terms of the motion trajectories (Figure 5), forces (Figure 4), and energetics (Figure 5). Further, we see that the pattern of forcing levels required at each step changes when the leg landing angle is changed. Steady state in the model was defined when the state parameters at touchdown and the

forcing were within 0.5% of the corresponding values for the periodic solution. The touchdown states are velocity (magnitude and direction) and step length and these are used to identify a periodic solution. For the solutions presented in Figure 4. (b-c), since there are large variations (approximately +130% to -85%) in the forcing between third and fourth step, and the forcing levels are significantly different than the forcing required at steady state, these solutions fail to capture the dynamics of gait initiation. However, in the forcing pattern shown in Figure 4 (d), the forcing levels at 3rd and 4th steps are <0.5% of the forcing required to achieve periodicity. This solution indicates a steady state has been reached by the third step. However, the forcing is high (0.15 BW compared to ~0.05 BW [25]) and the CoM trajectory does not resemble commonly observed patterns of CoM motion in a walking gait. Furthermore, the computed step lengths are larger than the experimentally observed step lengths (0.55 statures compared to ~0.42 statures[6]) suggesting that such solutions are not biologically realistic. Therefore, the next version of the model will also consider the initiation conditions created by the anticipatory postural adjustments.

2.3 Gait Initiation with Anticipatory Postural Adjustments (APAs):

In section 3.2, in the second study, we demonstrated that the model can achieve gait initiation with partial similarity to human experiments without including the CoM and CoP kinematics that result from the APAs that are observed in human studies. However, the model without APAs had forcing levels that varied widely between each step and the rotary force did not reach steady state for commonly observed leg landing angles within 4 steps.

Here, in a third study, we seek to determine if APAs can improve the performance of the bipedal SLIP model. The APAs lead to an initial movement of the CoP in the posterior direction creating an offset between the CoM and CoP. By the time of the first leg liftoff and start of gait

initiation, the CoM also achieves an initial velocity. To simply model the net effect of APAs we change the initial condition of the model's CoM by starting with a positive horizontal offset between the CoM and first foot position, and an initial forward velocity (which represents the effect of the initial backward motion of the CoP prior to the swing leg toe-off) (Figure 6). In contrast, the previous iteration of the model had the CoM vertically aligned with the CoP and at rest initially. Biologically relevant values for the initial offset and initial velocity at toe-off (at the start of motion) are approximated from [3,4,26]. Based on these, the results presented henceforth use an initial offset x_{CoM} between CoM and CoP approximated at 100mm and an initial velocity V_i approximated at 0.3 ms^{-1}.

Addition of APAs resulted in two important changes: (1) The landing angle at which steady state was achieved was 69.2° as compared to 61° in the absence of APAs (Figure 7). This can be concluded from the fact that the forcing at the third step onwards for both cases is < 0.5% of the forcing for the periodic solution. This is important because this new landing angle is in the commonly observed range from experimental results for nominal walking [27]. (2) The forcing pattern in the presence and absence of APAs for the same landing angle changed as well (Figure 7). The forcing which was oscillatory in the 3rd and 4th steps in the absence of APAs became nearly constant for those steps when APAs were included. As in the previous case, the per step rotary forcing sequence is fixed from the beginning of gait initiation. Further, in Figure 8 we show a comparison of the CoM trajectories with and without APAs at a landing angle of 69.2°. In the presence of APAs, the CoM reaches steady state in 4 steps whereas the CoM has yet to achieve steady state when effects from APAs were not considered.

At this point, it would be worthwhile to compare the kinematics obtained by the model to those observed experimentally which is shown in Figure 9. The characteristics of the velocity profile

are comparable, with the model reaching touchdown earlier than the experimental results (for the first step). The subsequent locomotion events of touchdown/heel contact and lift-off/toe-off occur at comparable periods.

The solution used as the representative case for this analysis was based on specific values selected for the initial conditions accounting for the effect of APAs. While these values are biologically representative, it is possible for them to vary. To further our understanding of the effect we computed some additional cases with various initial velocities. Figure 10 presents two of these cases in the immediate vicinity of the selected velocity. For a lower initial velocity, the solutions that reach a steady state within three steps have higer steady state forcing (0.9 BW [0.1 ms^{-1},65.7°] and 0.74 BW [0.2 ms^{-1},67.2°]vs 0.58 BW [0.3 ms^{-1}, 69.2°]).

2.4 Cost of Gait Initiation

Inclusion of APAs leads to a clear reduction in the CGI across all solutions, whether they represent steady state (third step onwards) or not (Figure 11). On comparison of the steady state solution along these two branches, a 57.9% reduction in CGI is obtained when APAs are considered. The comparison here is only for the solutions that reach steady state within the constraint of 4 steps.

2.5 Functional Relationship between Forcing and Speed:

Theoretical studies indicate that it is possible for humans and animals to achieve stable locomotion by proactively setting effective leg properties, or stated differently, the values of these effective leg properties are not changed during ensuing motion. Similarly, experimental studies conclude that gait initiation is a pre-programmed task consistent with feed-forward mode of neural control [11,22]. In context of the previously discussed modelling paradigm, this can be

presented as a feed-forward relationship between the actuation force and the velocity gain required to reach steady state. The information pertaining to the velocity at each step and hence the error with respect to steady state is available ahead of initiation. This can be related to the force calculated to achieve the intended velocity profile using a mathematical law which would allow the proactive calculation of the forces before the commencement of the initiation process. For the solution discussed in section 2.3 the variation of force and the difference in velocity during each step with respect to steady state is shown in Figure 12.

There are some interesting characteristics to be noticed here:

With an initial velocity of 0.3 ms^{-1}, the relationship between the forcing and velocity error is primarily linear. The following equation gives the functional relationship:

$$F_T = .128(\Delta v_i - \Delta v_3)^{.915} + .058$$

where velocity error Δv_i at i^{th} step is defined as

$$\Delta v_i = (v_{ref} - v_i)$$

Here v_{ref} is the target velocity (1.13 ms^{-1}), Δv_3 is the velocity error in the third step, right before steady state is achieved and v_i is the i^{th} step's velocity. It appears, in this case, that the relationship is close to a linear relationship given the value of exponent is ~1. However, the exponent coefficient varies with initial conditions. For the two other solutions reported in Figure 10, the equations are as follows:

0.1 ms^{-1}	$F_T = .049(\Delta v - \Delta v_3)^{.349} + .091$
0.2 ms^{-1}	$F_T = .064(\Delta v - \Delta v_3)^{.406} + .074$

These equations and the plots in Figure 12 clearly indicate that the distribution is sublinear in nature and conforms to a more general sublinear law as summarized by the following equation:

$$\text{Rotary Force}\,(F_T) = K_P(\Delta v_i - \Delta v_3)^{\alpha} + K_0 \qquad (1)$$

where K_0 is the constant forcing at steady state, and K_P is the proportional gain for the sublinear function. Some additional cases and analysis is presented in Appendix 5.3.

The above relationship suggests that for an intended velocity profile to be followed, it is possible to apply an averaged constant rotary force computed prior to gait initiation based on a closed form equation (as opposed to a numerical solution as in 2.2) to achieve the desired velocity. This relationship supports the experimental observation that gait initiation is a preprogrammed task where the actuation force is set for each step based on leg properties and APAs generated by the subjects (reflected in constants K_P, α and K_0). In contrast, if gait initiation was not an open-loop process, the force would have to be calculated at every instance of a step. The velocity error would have to be *sensed* at every instance whereas in open-loop, the velocity error and the intended force application is known at the start of the motion itself and no feedback is required.

3. DISCUSSION

In this paper, we develop a modeling framework to explore the transient process of gait initiation. We find that there is a strong correlation between the nature of forcing and the leg landing angle. Gait can be initiated with as simple a strategy as applying a constant rotary force. However, a change in force at each step allows the model to reach steady state speed in fewer steps. More importantly, the addition of APAs improves the performance of the model and results in gait initiation outcomes that are in agreement with experimental observations.

3.1 Importance of Anticipatory Postural Adjustments to process of Gait Initiation:

Inclusion of APAs in the model resulted in biologically relevant solutions. A comparison of the proposed solutions with and without APAs clearly show that the anticipatory actions lead

to a reduction in mechanical energy consumption (Figure 12), a decrease in step length (as the solutions move towards steeper landing angles) and a more natural CoM motion (Figure 5 (c) vs Figure 8) as observed experimentally for a walking gait.

The magnitude of the effect of APAs is also bounded. The initial displacement between the CoM and CoP is ~40% of the total displacement of CoM at first foot touchdown [3,4]. Also, the initial velocity achieved by the CoM before swing leg toe-off prior to the first step was ~50% of the average forward velocity during step 1 and ~ 25% of the velocity at swing leg touchdown at the end of the first step[3,4,26]. We chose to use the upper bounds for this body of work with the initial offset between CoM and CoP being 0.1 m and the initial velocity prior to the first step being 0.3 ms^{-1}. It would be challenging to experimentally manipulate the APA magnitude or to completely prevent them from occurring. However, patients with Parkinson's disease have shown a reduction in APAs due to deteriorated parasympathetic control of the TA and soleus muscles [12,28]. This leads to an associated loss of balance [12] and has been identified as one of the factors in the inability to achieve stable gait initiation. The results indicate that while it is possible to predict some of the kinematics of gait initiation in the absence of APAs, other characteristics like high forcing and increased step length (Figure 4(d)) are inconsistent with experimental observations. The results also suggest that to achieve more realistic step lengths (steeper landing angles), and achieve a steady state within three steps, APAs are needed to make a good prediction of the forcing. From a classical mechanics perspective, it makes sense that the initial moment produced by offset between CoM and CoP, and the momentum due to the velocity attained by the CoM, will change the nature of forcing required. In other words, the mechanical cost of gait initiation is decreased if the mass has initial momentum. The key understanding gained from the work presented here is regarding the nature of forcing required to

achieve gait initiation for selected leg properties like stiffness and landing angle. With or without including the effect of APAs, our model provides a unique solution where a unique pattern of applied force per step results in the CoM kinematics achieving steady state within 4 steps as observed in [6]. APAs help in reducing the effort required per step and in reaching steady state at steeper landing angles i.e. with shorter, more realistic step lengths. Furthermore, the qualitative similarity between the model's GRF and experimental GRF during steady state walking (Appendix 6.1) adds credibility to the model's overall behavior during the transient process of gait initiation as well.

3.2 Feed Forward Law:

An important result of this study is the ability to predict the required rotary forces ahead of time. Gait initiation has been shown to be a preprogrammed task [11,22], and the velocity progression profile through each step is primarily invariant across subjects of similar age group[6]. In support of this, the model predictions show that if the velocity profile is known ahead of time, the force required at each step can be computed in advance making for an open-loop relationship between force and velocity. If we consider the alternative, i.e. the force has to be computed at each instance throughout motion, based on the current velocity and the intended steady state velocity, we would get a standard closed loop system. From an implementation perspective, this would require constant feedback of the velocity. However, the model suggests that such a feedback law is not necessary to achieve the desired results and that a feed-forward law also predicts net averaged forces that need to be applied during each leg's stance phase to achieve the required velocity progression.

3.3 Model Limitations

The model used in this study has several limitations. Although the low dimensionality and

simplicity of the model enables analytical tractability, the model neglects many factors that could contribute additional effects in gait initiation behavior. For example, the leg properties like stiffness and damping used in the study are represented using very low fidelity functions, namely constants for each stance phase. In reality, however, there will be variations within the timeframe of one step that could contribute new effects, such as changes in peak forces. Here, we are focusing on the variation of leg properties at a time scale greater than a step, which can be pre-determined and enacted by a proactive control approach, in order to test hypotheses of what is possible with a simple proactive control approach and the ability for such a model to predict experimental outcomes.

The current model framework does not include a mechanistic model for the anticipatory postural adaptations (APAs), but rather a net effective model for APAs via an initial change to CoM position and velocity. Typically, forces associated with APAs are primarily radial in nature and are generated at the distal end of the foot by combined effects of activation of TA and the relaxation of soleus muscles[1,11,26]. Replicating this behavior is not possible in this model framework considering that the leg is massless and there is no actuation in the radial direction. Therefore, only kinematic after-effects of such adjustments are considered in the limited scope of the model parameters. The absence of a foot neglects another physical phenomenon, the translation of the CoP. Because of this, the force required to accelerate the CoM is expected to be higher in order to achieve comparable accelerations when CoP translation is considered. The first touchdown after initiation also happens earlier in stride phase (Figure 9) because the lack of translation of the CoP reduces the initial CoM translation as well. However, the horizontal CoM translations as well as the velocities at the end of first step are still comparable for the two cases based on Figure 9 and [27]. Lastly, the model assumes constant positive rotary forcing whereas

humans biologically exhibit both positive and negative joint moments. On closer inspection of the ground reaction forces (GRF) (Appendix 5.1) for the model it becomes evident that both positive and negative forces are present along the antero-posterior axis of motion. These cause the CoM to accelerate and decelerate. In future studies of the proactive dynamics of gait initiation, many additional complexities can be studied. Here, we believe we have discovered and validated a simple model that can correctly predict existing experimental data for gait initiation. Further, the model proposed here is relatively simple and easy to derive physical intuition from.

4. CONCLUSION

The focus of this paper was to understand the dynamics of gait initiation. To this effect, we were able to conclude that the dynamics of gait initiation are strongly related to the rotary forcing applied during stance. Furthermore, applying the same rotary force for every step in the gait initiation takes several more steps to reach steady state than what is observed experimentally. A step-by-step variation in forcing level allowed the model to reach steady state within the fixed constraint of 4 steps. However, it did not entirely agree well with experimental evidence. Most importantly, the model analysis provided insight into the importance and necessity of the anticipation phase of gait initiation where APAs generate momentum in walking direction. This resulted in a net reduction in the energetic cost of gait initiation, the forcing required at each step could be computed ahead of time and other behaviors like leg landing angle became biologically relevant and typical for human motion. The results of this study also help us understand how a compromised ability to generate APAs can lead to impairments in gait initiation, such as seen in Parkinson's disease. Finally, the model demonstrated that an open-loop approach can be used to compute the applied force based on the intended nature of motion, providing support to the experimental observation that gait initiation is a pre-programmed task.

5. APPENDIX:

5.1 Ground reaction forces at steady state:

A comparison of the vertical and horizontal ground reaction forces (GRF) between experimentally observed data and the model is presented in Figure 13. There are clear similarities and differences between the two. The qualitative behavior of the GRF are similar in these two cases. The vertical GRF exhibits the two peaks characteristic of experimentally observed GRF and the horizontal GRF has both negative and positive phases in the GRF providing deceleration and acceleration as observed experimentally. However, the GRF does not start from zero and there is a sharp change in the GRF at ~90% stride time when the second leg touches down. Also, the first peak in the vertical force is ~40% higher than experimental observations. The differences occur on account of the modeling choices of several parameters like stiffness, damping and rotary force being constant. It should be noted that a similar model for running with bilinear damping [29] successfully achieved similar GRF patterns as observed experimentally, with CoM motion and stability characteristics similar to those obtained with linear damping model used here.

5.2 Sensitivity to APAs:

The initial velocity achieved as a result of APAs was shown to have a significant effect on the nature of the forcing and the landing angle at which steady state is reached within the 4-step constraint, resulting in an overall reduction in energetic requirement. The contribution of APAs to the initial velocity was based on experimental observations [3,4]. Here we present more detailed analysis of how the force requirement changes as the initial velocity changes. Figure 14 details how the landing angle at which steady state is reached varies with initial velocity.

There is an increase in landing angle (reduction in step length) as the initial velocity increases. This also translates to a reduction in CGI (minimum CGI is achieved at an initial velocity of 0.35 ms^{-1}.)

A small increment in initial velocity due to APAs changes the nature of the forcing pattern. However, while it may be expected that an increase in APAs will correspond with a decrease in forcing throughout that is not always true. In particular, the force required at the first step increases. Since steady state is achieved at steeper landing angle (i.e. shorter step length), the propulsion phase for the first step is reduced while the system is still forced to achieve the same target velocity at the end of the first step, requiring increased forcing in the shorter duration.

5.3 Functional Relationship between Forcing and Speed:

This section aims at providing a feed-forward law that predicts the force required at each step. The functional relationship will be developed with respect to the velocity error from the steady state speed. As presented in the previous sections, there are multiple solutions that can be achieved based on the initial velocity achieved as a result of the APAs. In Figure 15, we present the variation in the force with velocity error for several of these initial conditions:
With an initial velocity of 0.3 ms^{-1}, the relationship between the forcing and velocity error is primarily linear.

The relationship for lower initial velocities is sublinear and superlinear for higher velocities. Table 2 enlists the functions corresponding to the initial conditions:

Initial Velocity (ms^{-1})	Forcing Function
0.1	$F_T = .049(\Delta v - \Delta v_3)^{.349} + .091$
0.2	$F_T = .064(\Delta v - \Delta v_3)^{.406} + .074$
0.3	$F_T = .128(\Delta v - \Delta v_3)^{.915} + .058$

0.4	$F_T = 1.959(\Delta v - \Delta v_3)^{3.385} + .043$

Table 2. relationship between rotary force and velocity error for different initial velocities achieved due to APAs.

6. COMPETING INTEREST

We have no competing interests.

7. AUTHORS' CONTRIBUTION

Manish Anand conducted the numerical simulations, analyzed and interpreted the results and drafted the manuscript, Justin Seipel conceived the study, helped in interpretation of results and drafted the manuscript, Shirley Rietdyk helped in interpretation of the results and helped draft the manuscript. All authors gave final approval for publication.

8. FUNDING STATEMENT

The study was partially supported by NSF Grant No. 1131423.

9. REFERENCES:

1. Brunt, D., Liu, S. M., Trimble, M., Bauer, J. & Short, M. 1999 Principles underlying the organization of movement initiation from quiet stance. *Gait Posture* **10**, 121–128. (doi:10.1016/S0966-6362(99)00020-X)
2. Brunt, D., Short, M., Trimble, M. & Liu, S. M. 2000 Control strategies for initiation of human gait are influenced by accuracy constraints. *Neurosci. Lett.* **285**, 228–30. (doi:10.1016/S0304-3940(00)01063-6)
3. Winter, D. A., Gilchrist, L., Jian, Y., Winter, D. A., Ishac, M. & Gilchrist, L. 1993 Trajectory of the body COG and COP during initiation and termination of gait. *Gait Posture* , 9–22.
4. Brenière, Y. & Do, M. C. 1991 Control of gait initiation. *J. Mot. Behav.* **23**, 235–40. (doi:10.1080/00222895.1991.9942034)
5. Polcyn, A. F., Lipsitz, L. a, Kerrigan, D. C. & Collins, J. J. 1998 Age-related changes in the initiation of gait: degradation of central mechanisms for momentum generation. *Arch. Phys. Med. Rehabil.* **79**, 1582–1589. (doi:10.1016/S0003-9993(98)90425-7)
6. Muir, B. C., Rietdyk, S. & Haddad, J. M. 2014 Gait initiation: the first four steps in adults aged 20-25 years, 65-79 years, and 80-91 years. *Gait Posture* **39**, 490–4. (doi:10.1016/j.gaitpost.2013.08.037)
7. Breniere, Y. & Do, M. C. 1986 When and how does steady state gait movement induced from upright posture begin? *J. Biomech.* **19**. (doi:10.1016/0021-9290(86)90120-X)
8. Najafi, B., Miller, D., Jarrett, B. D. & Wrobel, J. S. 2010 Does footwear type impact the number of steps required to reach gait steady state?: An innovative look at the impact of foot orthoses on gait initiation. *Gait Posture* **32**, 29–33. (doi:10.1016/j.gaitpost.2010.02.016)
9. Hwa-ann, C. & Krebs, D. E. 1999 Dynamic balance control in elders: Gait initiation assessment as a screening tool. *Arch. Phys. Med. Rehabil.* **80**, 490–494. (doi:10.1016/S0003-9993(99)90187-9)
10. Fortin, A. P., Dessery, Y., Leteneur, S., Barbier, F. & Corbeil, P. 2015 Effect of natural trunk inclination on variability in soleus inhibition and tibialis anterior activation during gait initiation in young adults. *Gait Posture* **41**, 378–383. (doi:10.1016/j.gaitpost.2014.09.019)
11. MacKinnon, C. D. C., Bissig, D., Chiusano, J., Miller, E., Rudnick, L., Jager, C., Zhang, Y., Mille, M.-L. & Rogers, M. W. 2007 Preparation of anticipatory postural adjustments prior to stepping. *J. Neurophysiol.* **97**, 4368–4379.
12. Sharma, S., Mcmorland, A. J. C. & Stinear, J. W. 2015 Stance limb ground reaction forces in high functioning stroke and healthy subjects during gait initiation. *Jclb* **30**, 689–695. (doi:10.1016/j.clinbiomech.2015.05.004)
13. Farley, C. T., González, O. & Gonzalez, O. 1996 Leg stiffness and stride frequency in human running. *J. Biomech.* **29**, 181–186. (doi:10.1016/0021-9290(95)00029-1)
14. Novacheck, T. 1998 The biomechanics of running. *Gait Posture* **7**, 77–95.
15. Geyer, H., Seyfarth, A. & Blickhan, R. 2006 Compliant leg behaviour explains basic dynamics of walking and running. *Proc. Biol. Sci.* **273**, 2861–7. (doi:10.1098/rspb.2006.3637)
16. Seipel, J. & Holmes, P. 2007 A simple model for clock-actuated legged locomotion. *Regul. chaotic Dyn.* **12**, 502–520. (doi:10.1134/S1560354707050048)
17. Shen, Z., Larson, P. & Seipel, J. 2013 Comparison of Hip Torque and Radial Forcing

Effects on Locomotion Stability and Energetics. In *Volume 6B: 37th Mechanisms and Robotics Conference*, pp. V06BT07A067. ASME. (doi:10.1115/DETC2013-13516)
18. Shen, Z. H. & Seipel, J. E. 2012 A fundamental mechanism of legged locomotion with hip torque and leg damping. *Bioinspir. Biomim.* **7**, 46010. (doi:10.1088/1748-3182/7/4/046010)
19. Seyfarth, A. 2003 Swing-leg retraction: a simple control model for stable running. *J. Exp. Biol.* **206**, 2547–2555. (doi:10.1242/jeb.00463)
20. Shen, Z. H., Larson, P. L. & Seipel, J. E. 2014 Rotary and radial forcing effects on center-of-mass locomotion dynamics. *Bioinspir. Biomim.* **9**, 36020. (doi:10.1088/1748-3182/9/3/036020)
21. Saranli, U. 2001 RHex: A Simple and Highly Mobile Hexapod Robot. *Int. J. Rob. Res.* **20**, 616–631. (doi:10.1177/02783640122067570)
22. Fiolkowski, P., Brunt, D., Bishop, M. & Woo, R. 2002 Does postural instability affect the initiation of human gait? *Neurosci. Lett.* **323**, 167–70. (doi:10.1016/S0304-3940(02)00158-1)
23. Blum, Y., Lipfert, S. W., Rummel, J. & Seyfarth, a 2010 Swing leg control in human running. *Bioinspir. Biomim.* **5**, 26006. (doi:10.1088/1748-3182/5/2/026006)
24. Zhang, L., Xu, D., Makhsous, M. & Lin, F. 2000 Stiffness and viscous damping of the human leg. *Proc. 24th Ann. Meet. Am. Soc. Biomech.,Chicago,* , 3–4.
25. Nilsson, J. & Thorstensson, a 1989 Ground reaction forces at different speeds of human walking and running. *Acta Physiol. Scand.* **136**, 217–27. (doi:10.1111/j.1748-1716.1989.tb08655.x)
26. Lepers, R. & Brenière, Y. 1995 The role of anticipatory postural adjustments and gravity in gait initiation. *Exp. Brain Res.* **107**, 118–124. (doi:10.1007/BF00228023)
27. Lee, C. R. & Farley, C. T. 1998 Determinants of the center of mass trajectory in human walking and running. *J. Exp. Biol.* **201**, 2935–44.
28. Halliday, S. S. E. et al. 1998 The initiation of gait in young, elderly, and Parkinson's disease subjects. *Gait Posture* **8**, 8–14. (doi:10.1016/S0966-6362(98)00020-4)
29. Abraham, I., Shen, Z. & Seipel, J. 2015 A Nonlinear Leg Damping Model for the Prediction of Running Forces and Stability. *J. Comput. Nonlinear Dyn.* **10**, 51008. (doi:10.1115/1.4028751)
30. Hamill, J., Bates, B. T. & Knutzen, K. M. 1984 Ground Reaction Force Symmetry during Walking and Running. *Res. Q. Exerc. Sport* **55**, 289–293. (doi:10.1080/02701367.1984.10609367)

Images:

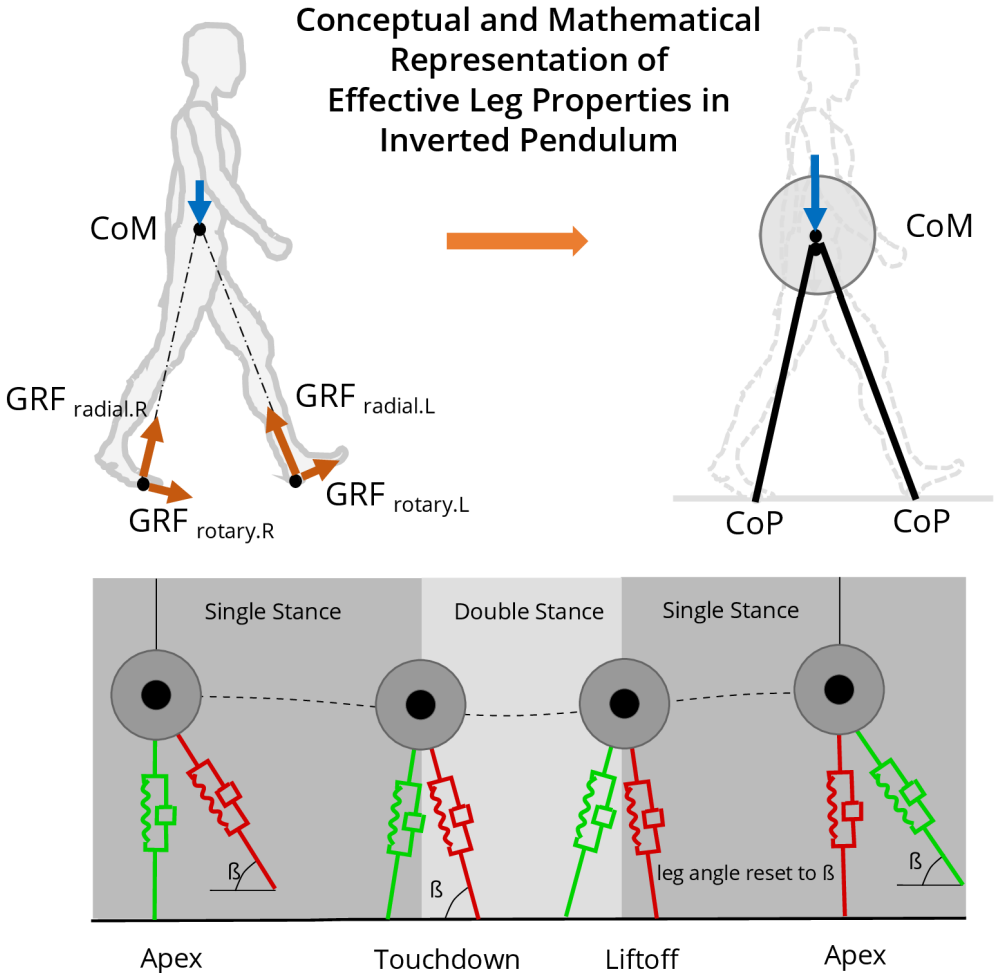

Figure 1**.** (Top row) Illustration of human locomotion dynamics. A polar frame of reference is defined for each leg by a line from the Center of Pressure (CoP) to the Center of Mass (CoM). "GRF" stands for Ground Reaction Force; "R" for the right leg; "L," left leg. The leg placement angle β is defined as the angle between the line from CoM to CoP and the horizontal frame of reference at foot touchdown (shown as left limb). The effective properties of the leg are represented mathematically, and abstractly as a viscoelastic spring leg that is placed at a desired angle upon touchdown. This spring leg interacts with the body, via a net effective joint moment (approximately a hip torque) to produce a force perpendicular to the radial direction from CoP to

the CoM. (bottom row) An abstract representation of an actuated and damped bipedal SLIP model, with single and double stance phases indicated. The swing leg angle is reset to a specified angle for touchdown. The translation of CoP is neglected in this model

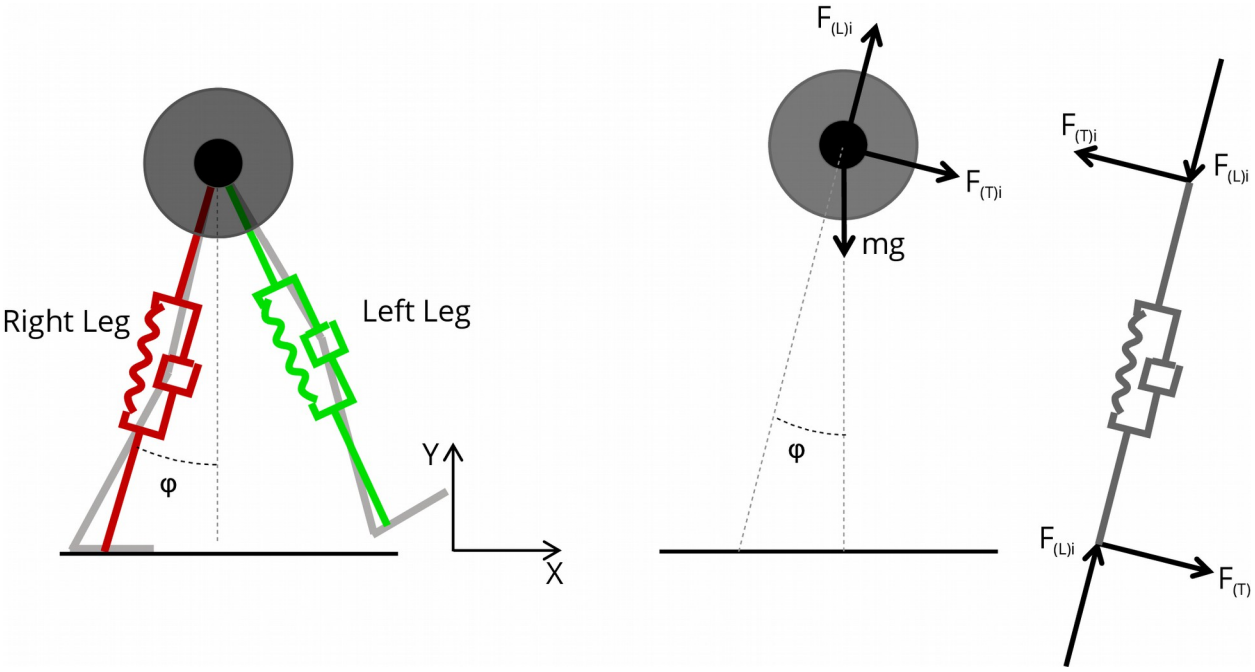

Figure 2. Schematic of the orientation of the forces acting on the CoM with one leg in stance and the other leg in swing phase. The representative leg segments of thigh, lower leg and foot are shown on left with the compliant leg representation superimposed on top.

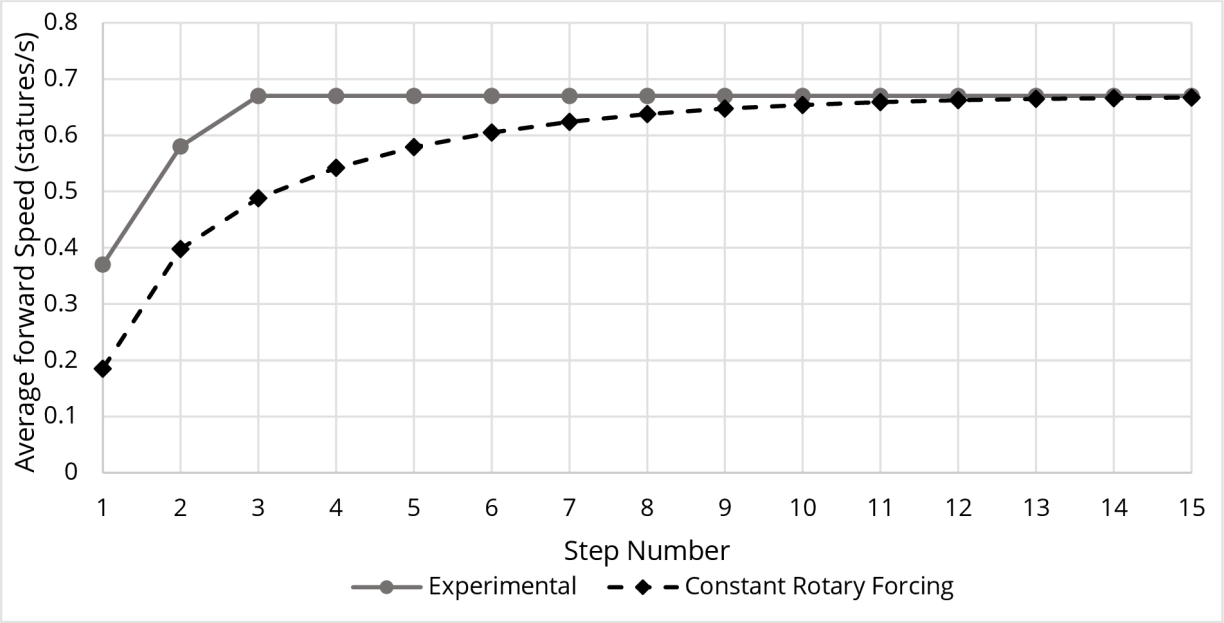

Figure 3. A comparison of the number of steps taken to achieve steady state with constant forcing to experimentally observed number of steps [6]. ζ=0.34; K_{REL}=29; β =70°

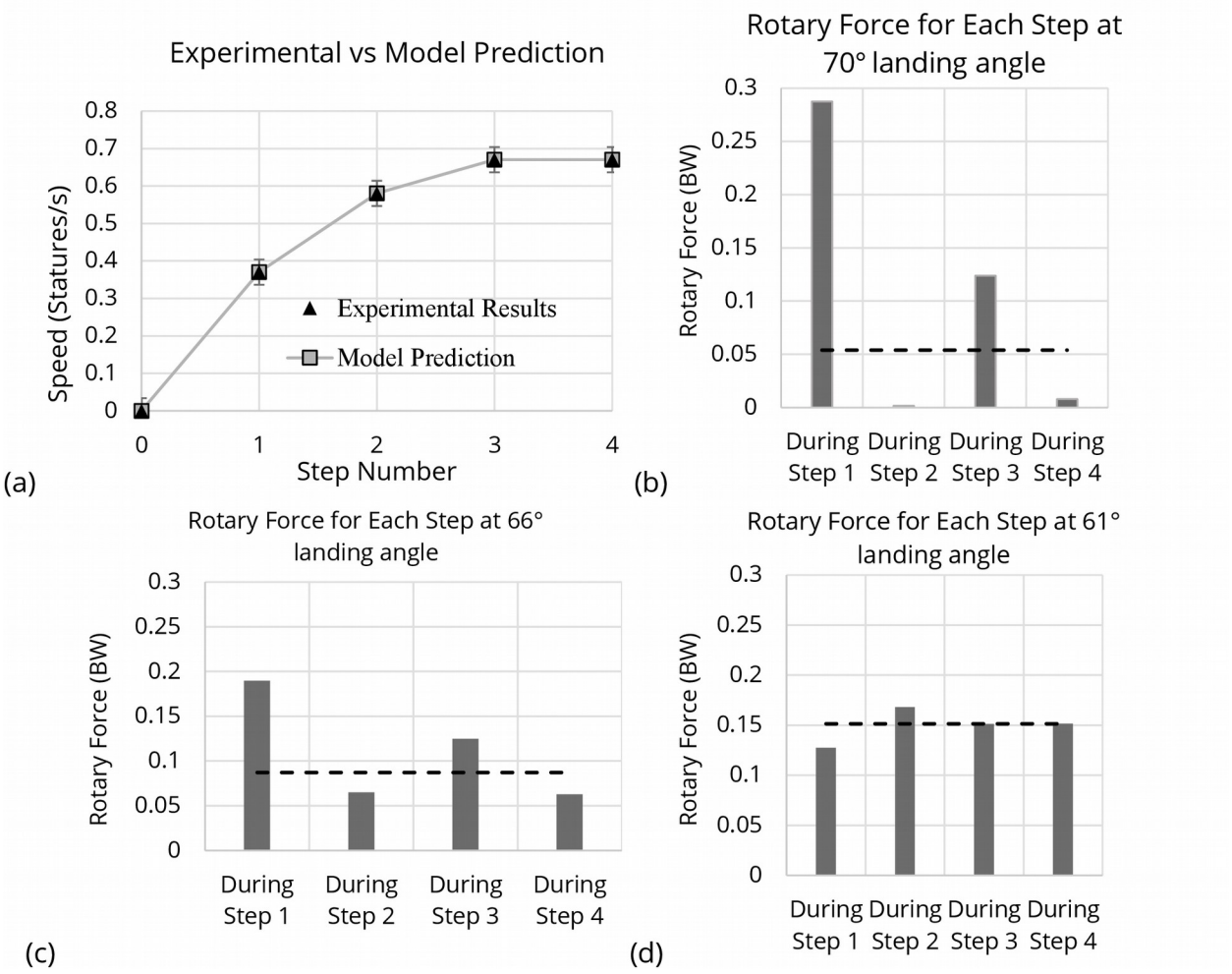

Figure 4. (a) Velocity profile achieved by the model when per step forcing changes as per (b),(c) or (d) exactly follows the experimental velocity profile [6]. (b), (c) and (d) Rotary forcing required at each step to generate the velocity profile in (a) at landing angles of 70°, 66° and 61° respectively. The horizontal line on these plots shows the forcing required at steady state to maintain steady state.

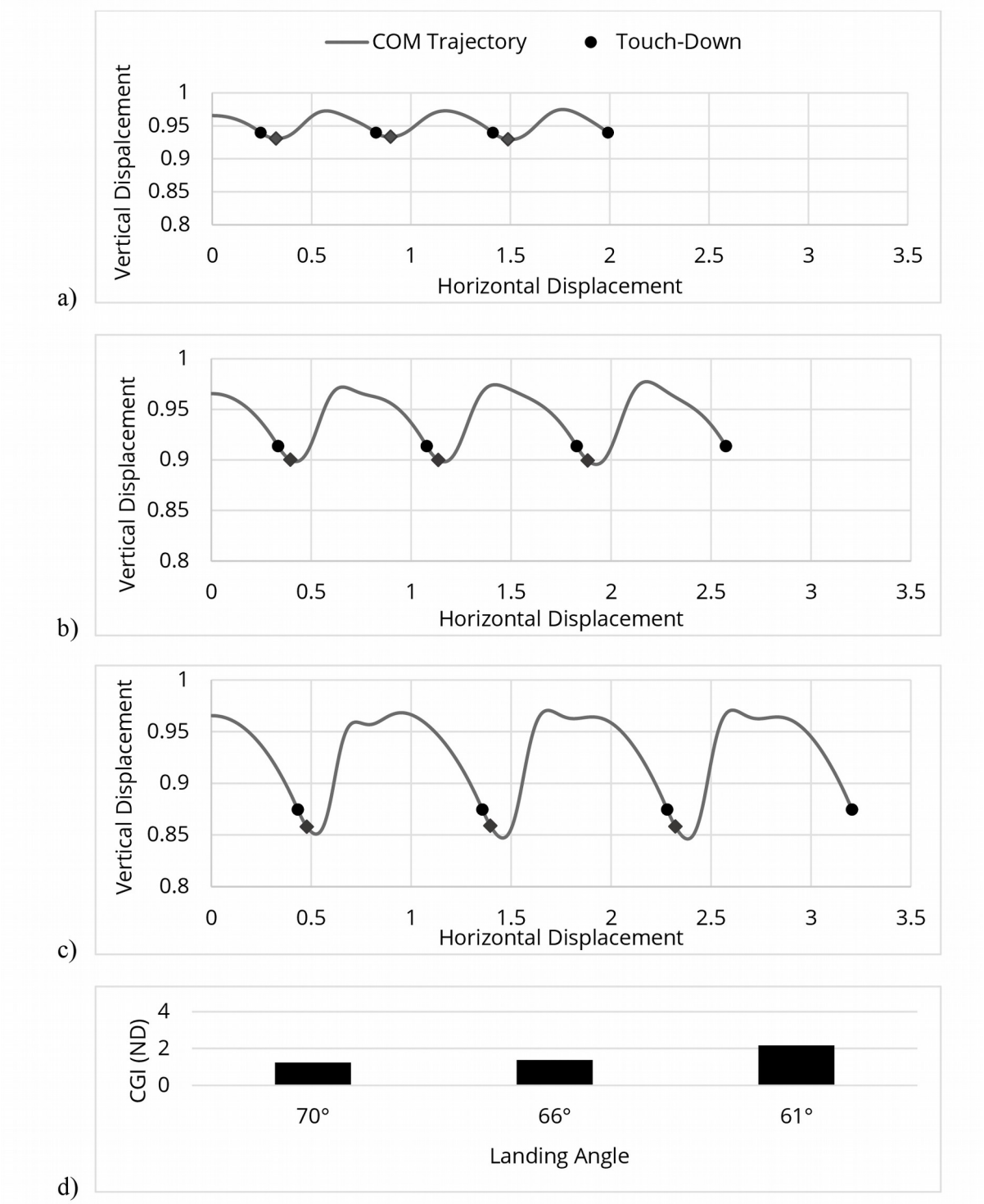

Figure 5. The non dimensionalized (ND) trajectory for center of mass (CoM) motion at (a) 70° and (b) 66° and (c) 61° is shown here. (d) Comparison of cost of gait initiation (CGI (ND)) for the three solutions.

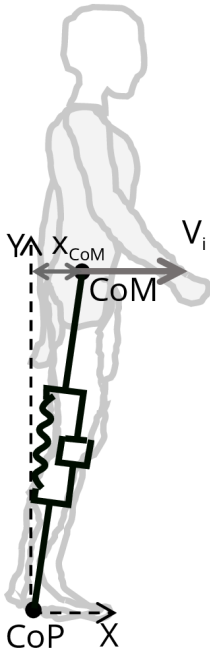

Figure 6. Model representation of the net effect of APAs.

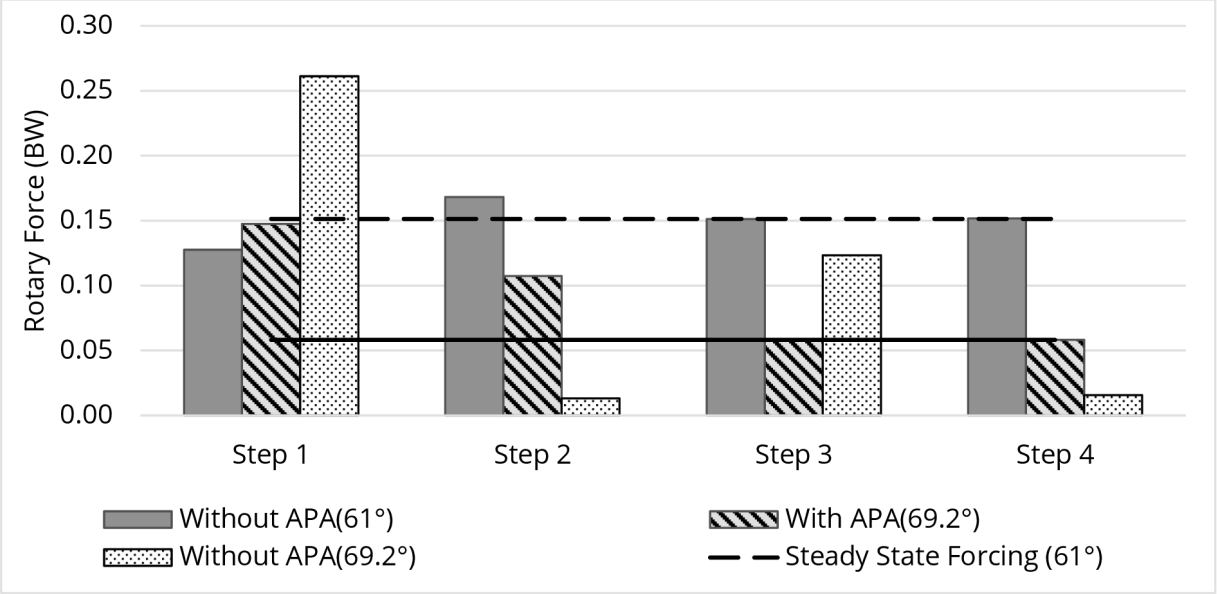

Figure 7. A comparison of the solution that reaches steady state (69.2°) in the presence of APAs to two solutions without APAs. In the absence of APAs steady state is achieved at (61°) as shown. For comparison, the solutions at (69.2°) is also presented without APAs indicating the impact on forcing that APAs have for invariant landing angles. Given enough steps (>10) this solution will eventually converge to steady state forcing as well. Steady state forcing is identified by the horizontal lines for the two landing angles and remains invariant in the presence or absence of APAs

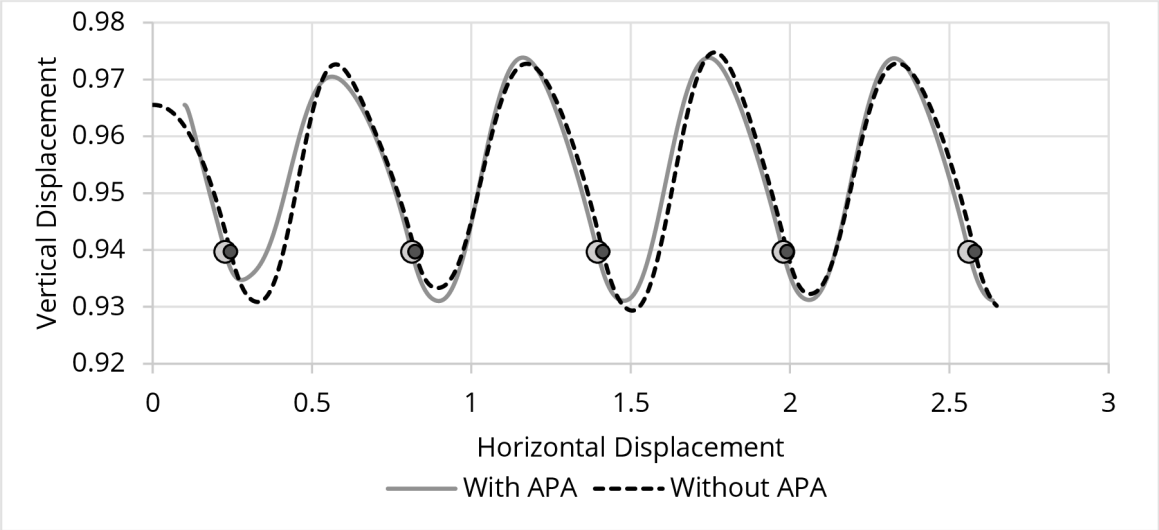

Figure 8. Comparison of the non-dimensional (ND) trajectories of CoM motion in the presence and absence of APAs. The touchdown events are marked (○) for each gait indicating the end of step.

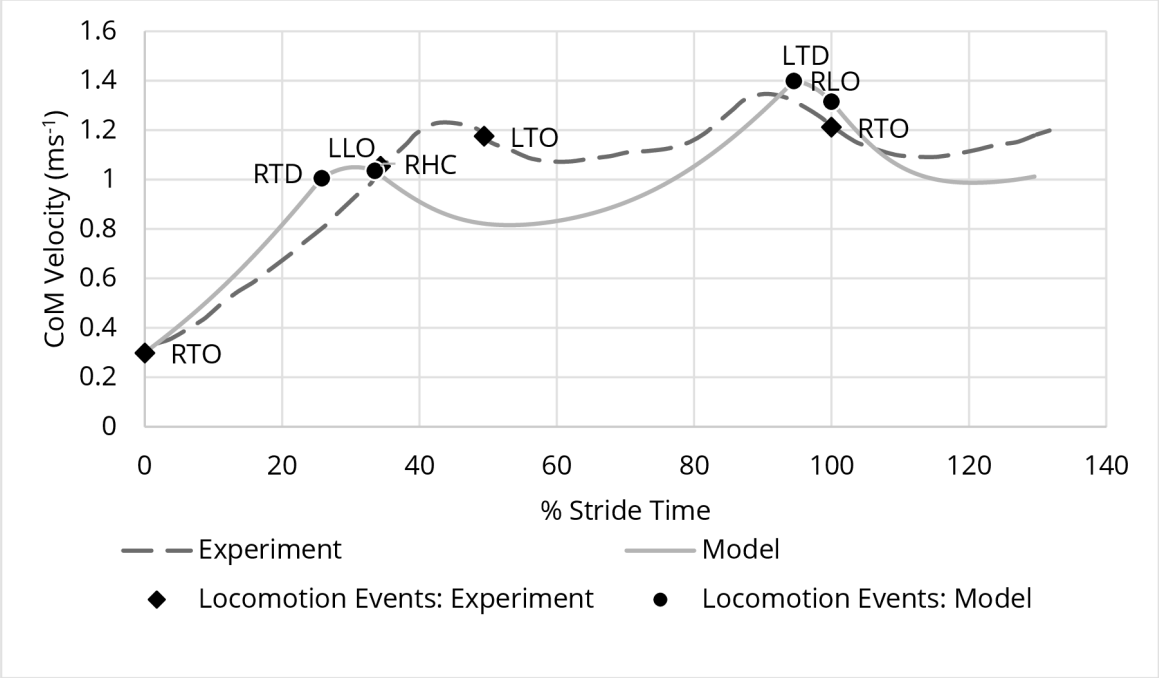

Figure 9. Comparison of experimental [3] and model CoM horizontal velocity profiles for one stride. Model events are identified as touch down(TD) and lift-off(LO) and experimental results are identified by (heel contact(HC) and toe-off(TO), for right (R) and left (L) legs.

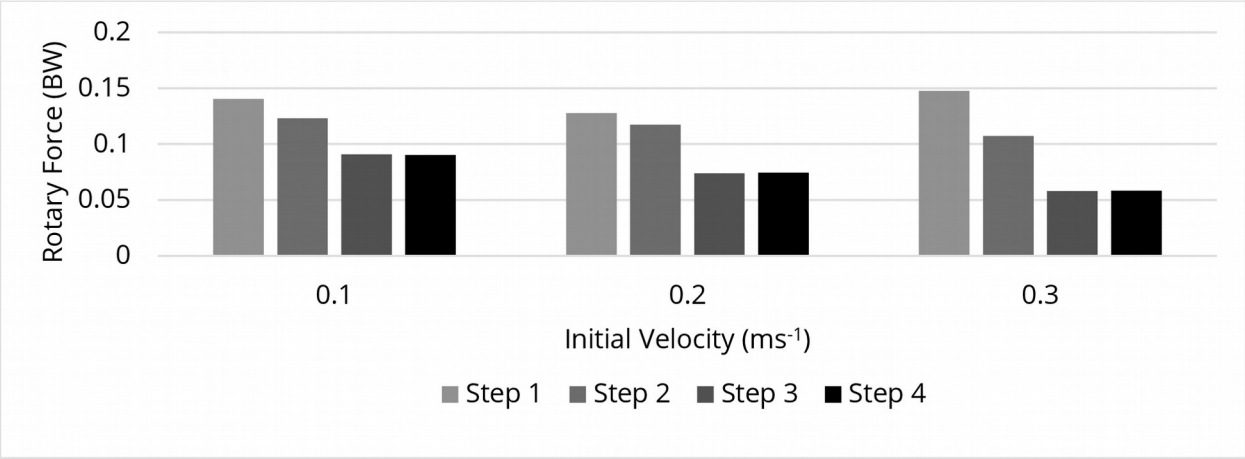

Figure 10. Forcing patterns for different initial velocities are presented for the solutions that reach steady state within 4 steps. The overall characteristic remains the same with a gradual decrease in the forcing per step. A detailed analysis is presented in Appendix 5.2 for a larger range of variation of initial velocity and resulting effects on energetics.

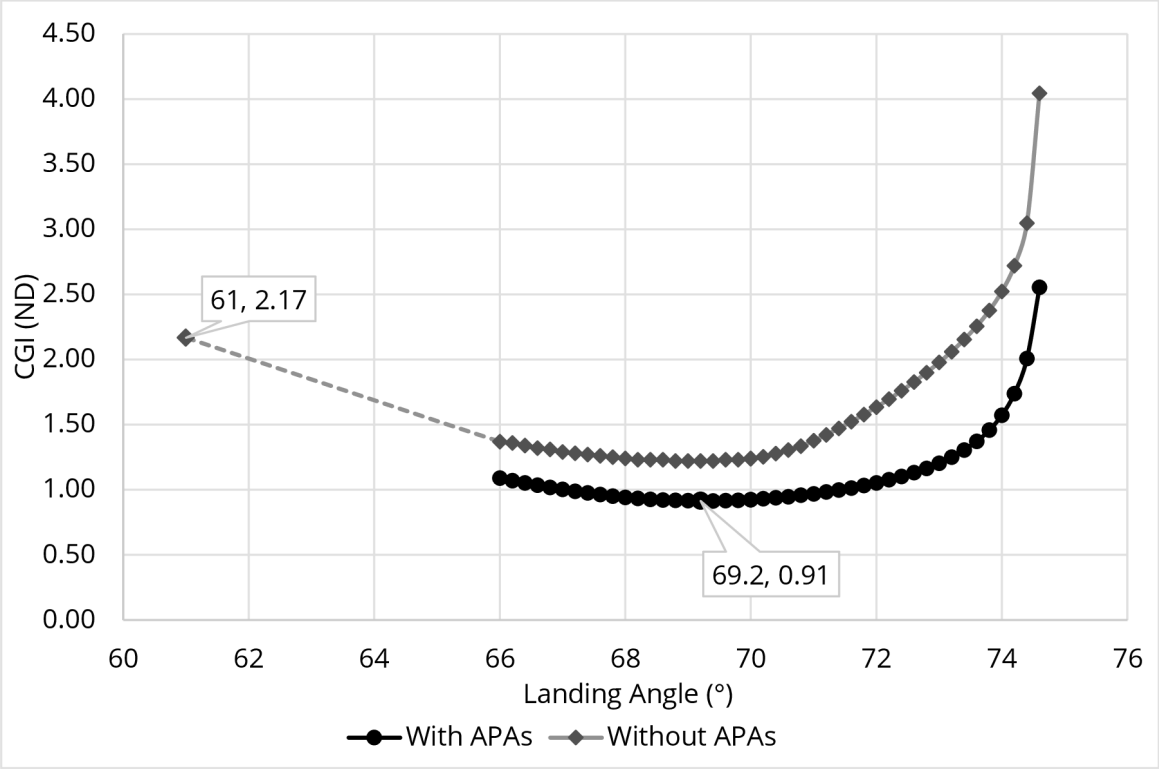

Figure 11. A comparison of Cost of Gait Initiation (CGI) across a range of landing angles with and without the effects of APAs added to the model. The CGI (ND) for the steady state solutions has been indicated on the plot for the two cases. The cases identified in the figure indicate that when APAs are considered, the steady state is achieved at 69.2° with a CGI of 0.91 (circle) while in absence of APAs, steady state is achieved at 61° with a CGI of 2.17(diamond).

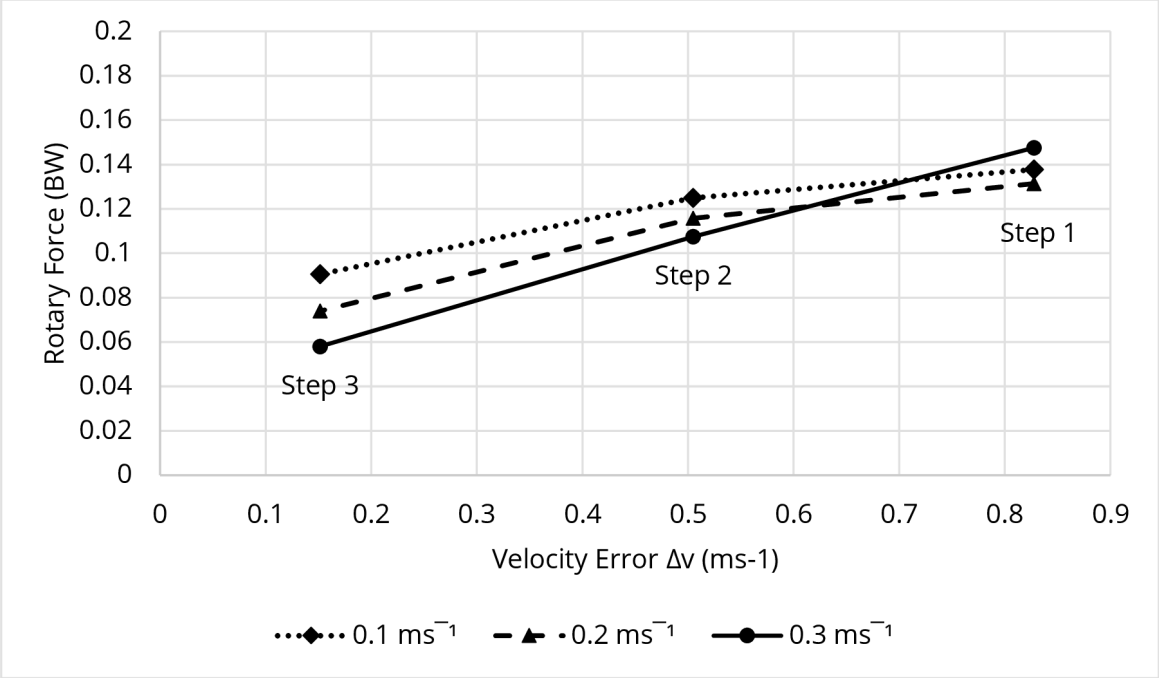

Figure 12. Relationship between forcing and velocity error for solution with anticipatory postural adjustments (APAs) (Section 2.3).

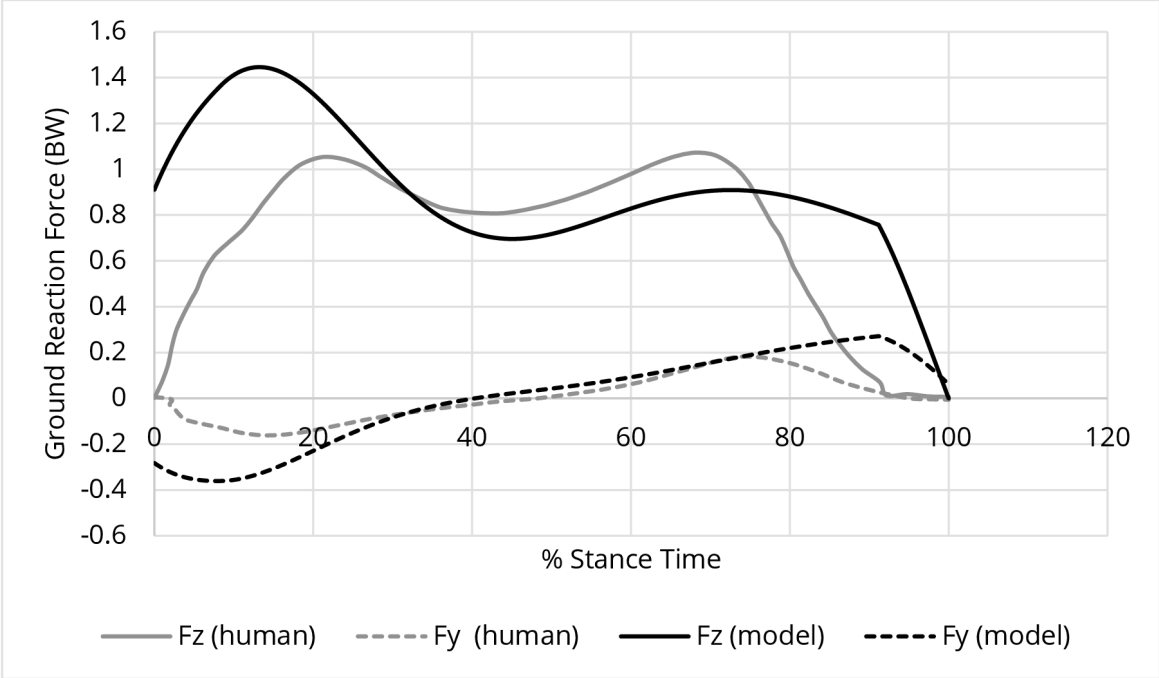

Figure 13. Comparison of the ground reaction forces between the model and human ([30]) (where Fz is vertical GRF and Fy is horizontal GRF)

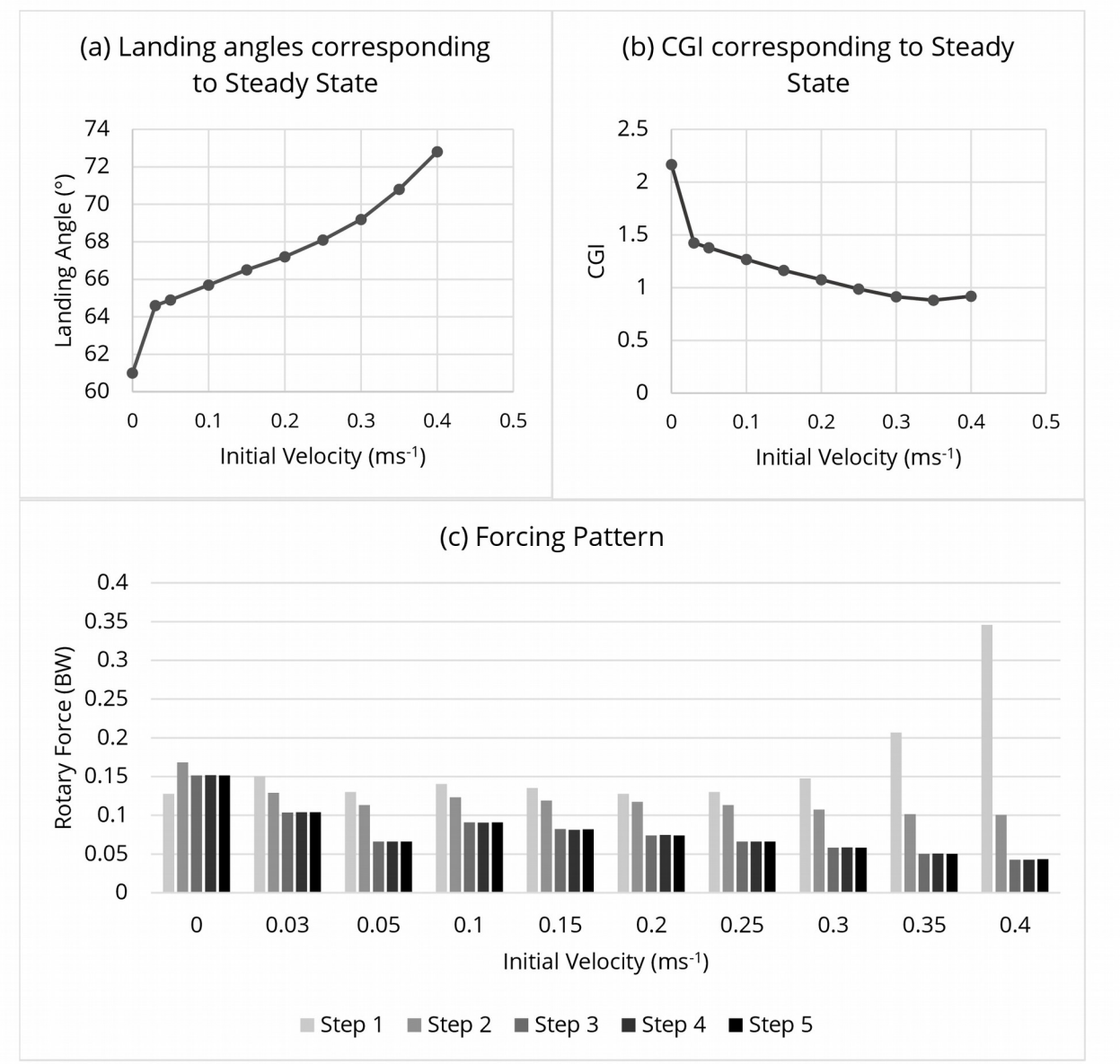

Figure 14. (a) shows the landing angles at which steady state is achieved corresponding to an initial velocity, (b) shows the CGI for the corresponding solutions and (c) shows the forcing patterns for 5 steps for these solutions.

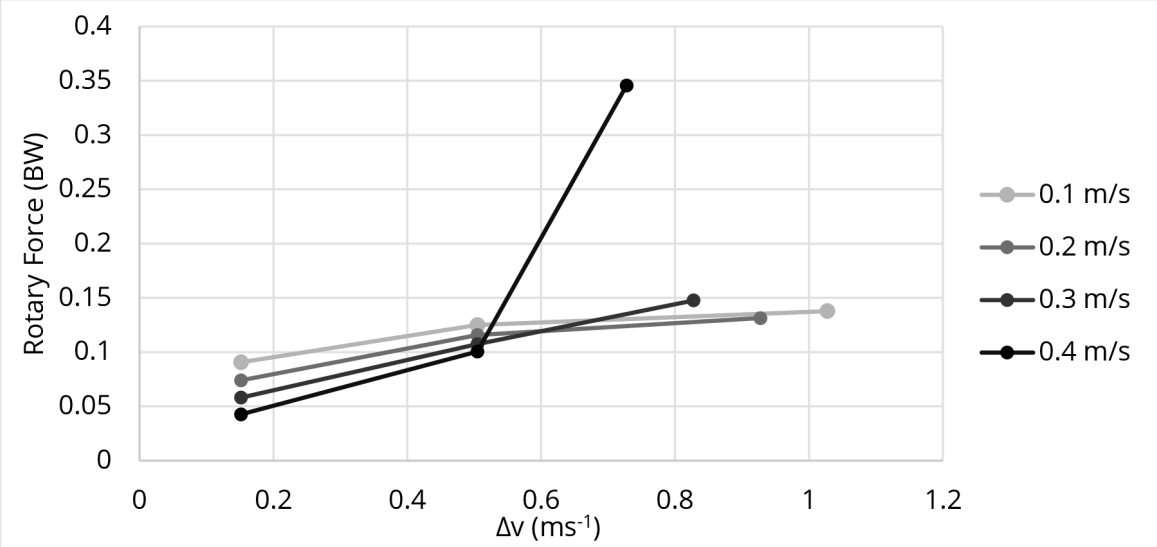

Figure 15. Functional relationship between forcing and velocity error for multiple initial velocities from 0.1 ms^{-1} to 0.4 ms^{-1}.